Nanosecond Fluorescence Decay Studies of the Deoxyribonucleic Acid–9-Aminoacridine and Deoxyribonucleic Acid–9-Amino-10-methylacridinium Complexes†

Yukio Kubota* and Yuko Motoda

ABSTRACT: The binding interaction of the mutagenic dye 9-aminoacridine (9AA) with DNAs of various base composition has been studied by steady-state and transient fluorescence measurements. It was found that the fluorescence decays of 9AA and 9AA bound to poly[d(A-T)] which contains only one type of binding site are single exponential but that those of 9AA bound to DNA can be well described as a sum of three-exponential functions. The fluorescence quantum yields confirm that the AT base pair is responsible for the fluorescence of the bound 9AA, while the GC base pair almost completely quenches it. Nanosecond time-resolved spectroscopy indicates that the structure of the DNA–9AA complex is not substantially altered during the lifetime of the excited singlet state of the dye. Furthermore, the fact that the shapes or the maxima of the absorption and fluorescence spectra exhibit no dependence on the GC content of DNA indicates that the radiative lifetime of the bound 9AA is constant under a variety of circumstances. On the basis of these results, it is concluded that the emitting sites of 9AA on DNA are composed of at least three classes having different quantum yields: (I) $\tau_1 = 2.0 \pm 0.3$ ns, $\phi_1 = 0.06 \pm 0.01$, (II) $\tau_2 = 12.3 \pm 0.7$ ns, $\phi_2 = 0.35 \pm 0.02$, and (III) $\tau_3 = 28.3 \pm 0.5$ ns, $\phi_3 = 0.81 \pm 0.02$. Fluorescence decay behavior is also reported for the nonmutagenic dye 9-amino-10-methylacridinium (10Me-9AA) bound to DNA. The results of 10Me-9AA were found to be very similar to those of 9AA.

The interaction of acridine dyes such as proflavin (PF)[1] and 9-aminoacridine (9AA) with DNA is of special interest because of their strong mutagenic activity (Orgel & Brenner, 1961). It is well established that there are two processes by which acridines bind to DNA (Peacocke & Skerrett, 1956): the strong binding process which predominates at a high molar ratio of DNA phosphate to dye (P/D) and the weak binding process which takes place at a low P/D value and arises from electrostatic interactions between the positive charge of the dye and the negative charge of the DNA phosphate. Lerman (1961, 1963) proposed that the strong binding of acridine dyes occurs by intercalation between adjacent base pairs. Excellent review articles on the subject have recently appeared (Peacocke, 1973; Lochmann & Micheler, 1973; Georghiou, 1977).

Optical methods, particularly fluorescence methods, are the most appropriate for a study of the binding interaction. Fluorescence quenching studies of the DNA–PF and DNA–acriflavin (10-methylated PF) complexes showed that there are two classes of strong binding sites (Tubbs et al., 1964; Thomes et al., 1969; Chan & McCarter, 1970; Pachman & Rigler, 1972; Weisblum & de Haseth, 1972; Kubota, 1973; Schreiber & Daune, 1974; Kubota et al., 1978). One class (GC base pair) almost completely quenches the fluorescence of the bound dye, while the other (AT base pair) does not alter its fluorescence quantum yield; the first is called quenching sites and the other is called emitting sites (Thomes et al., 1969). In a previous paper (Kubota et al., 1978), we reported that AT base pairs are responsible for the fluorescence of the bound 9AA as well as of the bound PF but that the quantum yield characteristics of the bound 9AA are different from those of the bound PF. That is, the fluorescence quantum yield of the bound PF linearly varies with the fraction of AT-AT sites, while that of the bound 9AA does not. This phenomenon may be attributed to the heterogeneity of emitting sites.

The heterogeneity of binding sites seems to be important for the understanding of the biological actions of acridine dyes (Schreiber & Daune, 1974). In order to clarify the nature of binding sites, we are undertaking a systematic investigation on the interaction of DNA with various acridine dyes by measuring fluorescence lifetimes and quantum yields (Kubota, 1973; Kubota & Steiner, 1977a,b; Kubota & Fujisaki, 1977; Kubota et al., 1978, 1979a). A combination of nanosecond time-resolved spectroscopy and steady-state fluorescence techniques will allow us to obtain a deeper insight into the nature of binding sites.

Duportail et al. (1977) have recently shown that fluorescence decay curves of several acridine dyes upon binding to DNA can be resolved into two-exponential components. On the other hand, our preliminary results have revealed that the fluorescence decay of 9AA bound to DNA does not follow a two-exponential decay law but that the data can be well described as a sum of three-exponential functions (Kubota et al., 1979a).

Here we report a detailed study on the decay kinetics of the DNA–9AA complexes and also report a comparison of results for 9AA with those for 9-amino-10-methylacridinium chloride (10Me-9AA) which has no mutagenicity (Lerman, 1964). The decay behavior was found to be complex, and possible interpretations are discussed in connection with the nature of emitting sites.

Materials and Methods

Bacteriophage T2 DNA was prepared by the method of Mandell & Hershey (1960). The following DNAs and synthetic polynucleotides were commercial products: *Clostridium perfringens* DNA (CP DNA; Worthington), calf thymus DNA (CT DNA; Worthington), *Escherichia coli* DNA (EC DNA;

† From the Department of Chemistry, Faculty of Science, Yamaguchi University, Yamaguchi 753, Japan. *Received January 14, 1980.* This work was supported by a grant-in-aid for Scientific Research from the Ministry of Education of Japan.

[1] Abbreviations used: PF, proflavin; 9AA, 9-aminoacridine; 10Me-9AA, 9-amino-10-methylacridinium chloride; TPB, 1,1,4,4-tetraphenyl-1,3-butadiene; CP DNA, *Clostridium perfringens* DNA; CT DNA, calf thymus DNA; EC DNA, *Escherichia coli* DNA; ML DNA, *Micrococcus lysodeikticus* DNA; P/D, molar ratio of DNA phosphate to dye.

0006-2960/80/0419-4189$01.00/0

Worthington), *Micrococcus lysodeikticus* DNA (ML DNA; Miles), poly[d(A-T)] (Miles), and poly(dG)·poly(dC) (Miles). Denatured DNA was prepared by heating a DNA solution for 20 min in boiling water, followed by rapid cooling in ice–water. 9AA was the same sample as used before (Kubota et al., 1978, 1979a). 10Me-9AA was prepared according to the method of Albert & Ritchie (1943) and was purified by repeated recrystallizations from hot water until no trace of the unreacted 9AA was detected by the method of thin-layer chromatography. Glass-redistilled water was used for all measurements. All chemicals were of reagent grade or better.

Absorption and steady-state fluorescence spectra were recorded with a Shimadzu UV-200S spectrophotometer and a Hitachi MPF-2A spectrophotofluorometer, respectively, using quartz cells of 1-cm path length. For fluorescence measurements, the excitation monochromator was set at 390 and 400 nm for 9AA and 10Me-9AA systems, respectively, with a 3–6-nm band-pass, and the emission was recorded with a 2–3-nm band-pass. Dye concentrations were in the range 8–13 μM, thus ensuring that the maximum absorbance at the excitation wavelength did not exceed 0.05. The spectra recorded at the highest sensitivity of the fluorometer were corrected for distortions by scattering. Complete fluorescence spectra were corrected for the unequal quantum response of the detector system which consists of lenses, a monochromator, and an R446-UR or an R106-UH photomultiplier tube (Hamamatsu TV). Fluorescence quantum yields were determined by considering the artifact due to the polarization and by comparing the area under the fluorescence spectrum of the complex with the corresponding area of 9AA or 10Me-9AA (Kubota & Steiner, 1977a; Kubota et al., 1978). The quantum yield of the dye was determined by using the standard reference, quinine sulfate in 1 N H_2SO_4 (Melhuish, 1961).

Fluorescence decay curves and nanosecond time-resolved fluorescence spectra were measured with an Ortec nanosecond emission spectrophotometer equipped with an RCA 8850 photomultiplier tube (Kubota et al., 1979a,b). All decay measurements were performed under single photon counting conditions. Excitation pulses from a flash lamp were passed through a Corning 7-60 filter or a 375-nm interference filter (Japan Vacuum Optics) and focused on the sample with a lens. The flash lamp was thyratron-triggered, air-filled (0.5 atm), and run at ~25 kHz. Emission from the sample cuvette was observed at right angles through a grating monochromator (Applied Photophysics Ltd.) with slit widths giving a 5–20-nm band-pass for decay measurements and a 5-nm band-pass for the time-resolved work. When fluorescence decays of the DNA–dye complexes were measured, care was taken to eliminate anisotropic contributions to the observed decay (Spencer & Weber, 1970; Shinitzky, 1972). This was done by exciting with an unpolarized beam of light and observing the fluorescence through a Polacoat polarizer whose axis was 54.7° to the excitation observation plane.

The observed fluorescence decay curve $i(t)$ is represented by the convolution integral:

$$i(t) = \int_0^t g(u)I(t-u)\,du \qquad (1)$$

where $g(t)$ is the apparatus response function and $I(t)$ is the fluorescence decay which would be obtained with the δ-pulse excitation. It has been shown that the response function $g(t)$ is dependent on the energy of the photon impinging on the photocathode (Wahl et al., 1974). According to the method of Wahl et al. (1974), the true $g(t)$ was determined from the fluorescence decay curve of 1,1,4,4-tetraphenyl-1,3-butadiene (TPB) in deaerated cyclohexane which has a single-exponential

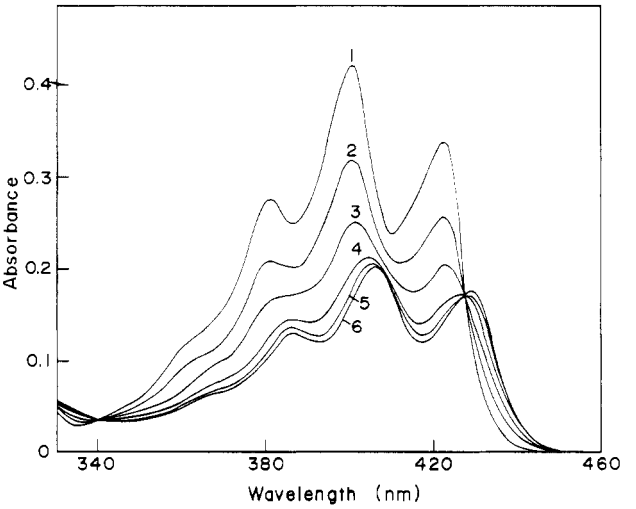

FIGURE 1: Absorption spectra of the CP DNA–9AA system in 5 mM phosphate buffer (pH 6.9) at 25 °C. 9AA: 44 μM. P/D: (1) 0; (2) 1.5; (3) 3; (4) 5; (5) 7; (6) above 20.

decay. The lifetime of TPB was determined with excitation and emission wavelengths set at 375 and 425 nm, respectively. Under these conditions, the wavelength effect is small and $g(t)$ could be determined by using a scattering solution (Gafni et al., 1975). The lifetime of TPB was found to be 1.72 ± 0.02 ns at 25 °C; this value is in good agreement with the value reported by Berlman (1971) (1.76 ns).

The fluorescence decay $I(t)$ was assumed to be a sum of exponential functions which could be written as

$$I(t) = \sum_{i=1}^{n}[\alpha_i \exp(-t/\tau_i)] \qquad (2)$$

where α_i and τ_i are the amplitude and lifetime, respectively, of the ith component. Decay parameters (α_i's and τ_i's) were obtained from deconvolution of eq 1 by using computer programs based on the method of nonlinear least squares (Grinvald & Steinberg, 1974) and/or on the method of Laplace transformation (Gafni et al., 1975). The fit between the observed and theoretical decay curves was evaluated by convolving the apparatus response function $g(t)$ with the decay parameters obtained by analyses and by inspection of the reduced χ^2, the weighed residuals, and the autocorrelation function of the residuals (Bevington, 1969; Grinvald & Steinberg, 1974; Gafni et al., 1975). Data analysis was accomplished by using a PDP 11/04 minicomputer (Digital Equipment Corp.) interfaced with an Ortec 6240B multichannel analyzer. The accuracy of the system's time scale was checked by calibrating the time-to-amplitude converter by an Ortec 462 time calibrator and by measuring the lifetime of quinine sulfate in sulfuric acid. These criteria indicated time-scale accuracy of 0.2 ns or better.

All measurements were made at 25 ± 0.1 °C under two solvent systems: 5 mM phosphate buffer (pH 6.9 and ionic strength of 0.01) and unbuffered NaCl solutions (0.001–0.4 M) in which pH was found to vary between 6.2 and 6.5.

Results

Absorption and Fluorescence Spectra. Figure 1 shows the absorption spectra of the CP DNA–9AA system as a function of P/D. The absorption bands can be seen to shift progressively toward a limit (curve 6) which represents the spectrum of 9AA in a fully complexed form. All the curves pass through isosbestic points at 340 and 427.5 nm, indicating that they result from the contributions of two forms of 9AA, free and

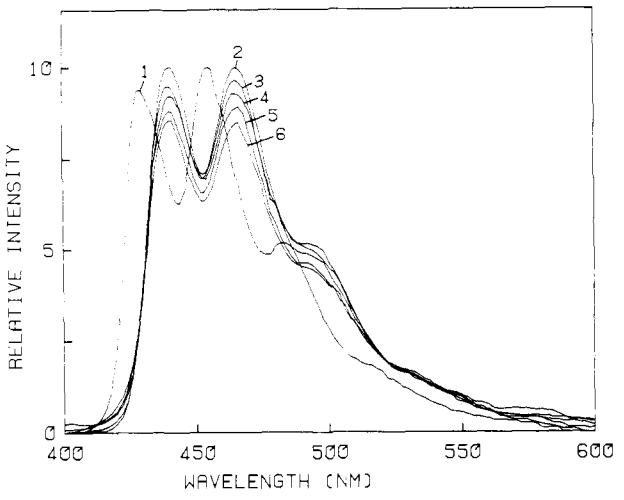

FIGURE 2: Fluorescence quantum spectra of 9AA (8–13 μM) in the presence of various DNAs in 5 mM phosphate buffer (pH 6.9) at 25 °C: (1) free; (2) poly[d(A-T)] (P/D = 136); (3) CP DNA (P/D = 400); (4) T2 DNA (P/D = 101); (5) CT DNA (P/D = 205); (6) EC DNA (P/D = 417). The excitation wavelength was 390 nm. The units of the ordinate are arbitrary; the maximum of each spectrum is properly reduced to avoid overlapping.

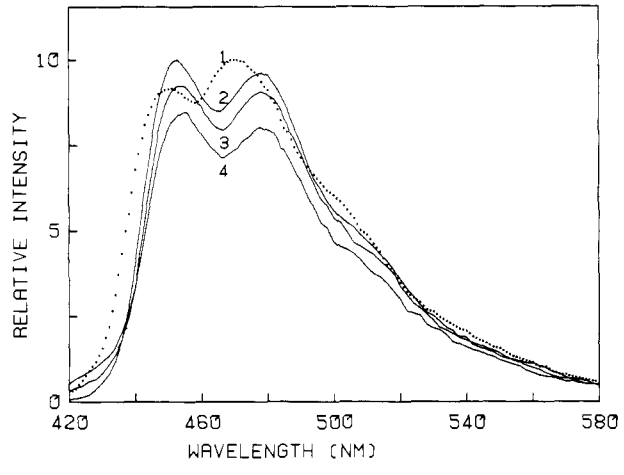

FIGURE 3: Fluorescence quantum spectra of 10Me-9AA (8–13 μM) in the presence of various DNAs in 5 mM phosphate buffer (pH 6.9) at 25 °C: (1) free; (2) poly[d(A-T)] (P/D = 141); (3) CP DNA (P/D = 200); (4) CT DNA (P/D = 400). The excitation wavelength was 400 nm.

bound, each form having a characteristic absorption spectrum. Very similar absorption changes were also obtained with 9AA complexed with other DNAs and synthetic polynucleotides [poly[d(A-T)] and poly(dG)·poly(dC)] and with the DNA–10Me-9AA complexes; the shapes or the maxima of the absorption spectra of the bound dye were independent of the GC content of DNA.

From Scatchard plots in which free and bound dye concentrations were calculated from spectrophotometric measurements (Peacocke & Skerrett, 1956), the apparent association constants (k_{app}) and the apparent numbers of available binding sites per DNA phosphate (n_{app}) were determined in 5 mM phosphate buffer at 25 °C. The k_{app} values for 9AA and 10Me-9AA upon binding to DNA (Table I) or synthetic polynucleotides (Table II) were of the same order of magnitude [$(0.9–1.6) \times 10^6$ M^{-1}], showing almost no dependence on the base composition of DNA. The n_{app} values were found to be 0.22–0.24 for DNA and poly[d(A-T)] and 0.20 for poly(dG)·poly(dC).

Figures 2 and 3 indicate the fluorescence spectra of 9AA and 10Me-9AA, respectively, in the presence of various DNAs

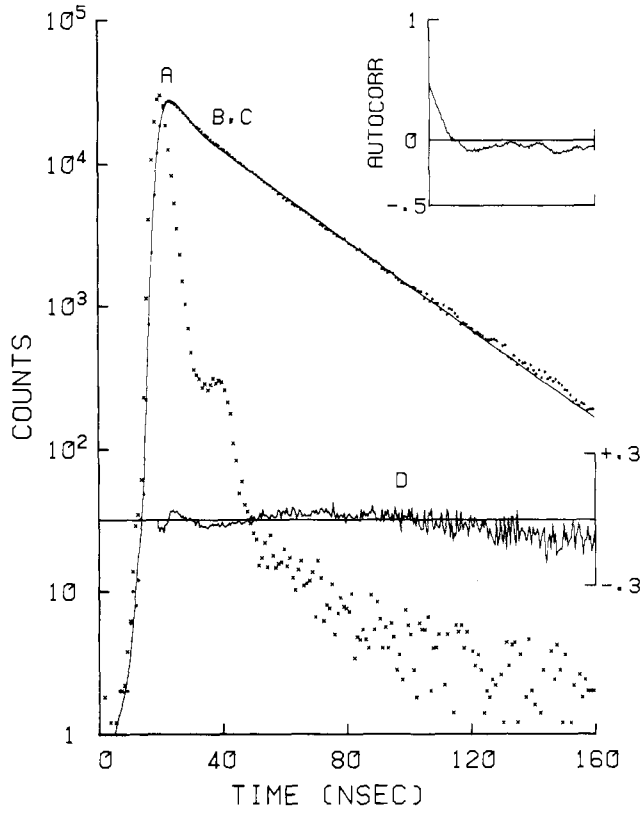

FIGURE 4: Two-component analysis of the fluorescence decay of the CP DNA–9AA complex (P/D = 201) in 5 mM phosphate buffer (pH 6.9) at 25 °C. The concentration of 9AA was 13 μM, and the decay was observed at 455 nm. Curve A is the apparatus response function. Curve B is the observed decay curve. The smooth curve C shows the computed decay curve. Curve D is the weighed residuals. The inset is the autocorrelation function of the residuals. Parameters obtained: τ_1 = 4.2 ns, τ_2 = 27.3 ns, α_1 = 0.144, α_2 = 0.151, and χ^2 = 4.34. The amplitudes normalized to unity are α_1 = 0.49 and α_2 = 0.51.

at high P/D values where the concentration of the free dye is negligibly small. The shape or the maximum of the fluorescence spectrum of the dye bound to DNA can be seen to be almost identical with that of the dye bound to poly[d(A-T)], regardless of the GC content of DNA. On the other hand, the fluorescence quantum yield of the dye bound to DNA (ϕ) strongly depended on the base composition; the value of ϕ decreases with increasing GC content and is almost zero in the case of poly(dG)·poly(dC) (Tables I and II). These findings suggest that AT base pairs of DNA are responsible for the fluorescence of the bound dye, and GC base pairs almost completely quench it (Kubota & Fujisaki, 1977; Kubota et al., 1978).

Fluorescence Decay Curves. In order to obtain further information on the interaction between the dye and the binding sites, we investigated transient fluorescence decay curves of 9AA and 10Me-9AA upon binding to DNAs of various base composition. Decay measurements were made at high P/D values (P/D > 100) and at low ionic strength (5 mM phosphate buffer) to minimize the effect of unbound dye. Under these conditions, the contribution of free dye was estimated, by using k_{app} and n_{app}, to be below 0.3% (Table I); dialysis experiments also showed that the concentration of unbound dye was extremely small compared to that of bound dye.

It was found that the fluorescence decay kinetics of the dye followed a single-exponential decay law but that of the dye bound to DNA was complex. Typical decay curves obtained with the CP DNA–9AA complex (P/D = 201) are shown in Figures 4 and 5. Figure 4 shows the best fit for a two-ex-

Table I: Fluorescence Decay Parameters and Quantum Yields for 9AA, 10Me-9AA, and Their Complexes with DNAs of Various Base Composition[a]

system	GC (%)	$k_{app} \times 10^{-6}$ (M^{-1})	P/D	free dye[b] (%)	τ_1	α_1	τ_2	α_2	τ_3	α_3	ϕ
9AA					15.8	1.00					0.960
CP DNA-9AA	30	1.4	101	0.23	2.3	0.38	11.8	0.24	28.0	0.38	0.126
			150	0.15	2.4	0.37	12.7	0.23	28.6	0.40	0.126
			201	0.11	2.2	0.40	12.2	0.22	29.2	0.38	0.131
			400	0.06	2.1	0.39	12.3	0.21	28.9	0.40	0.129
T2 DNA-9AA	34	1.6	101	0.20	2.1	0.51	12.9	0.19	28.5	0.30	0.088
			202[c]	0.10	2.4	0.52	13.1	0.17	28.4	0.31	0.090
			404	0.05	2.2	0.51	12.8	0.17	28.6	0.32	0.090
CT DNA-9AA	42	1.0	103	0.31	1.9	0.58	12.5	0.15	28.1	0.27	0.043
			205	0.15	1.7	0.58	11.5	0.14	28.3	0.28	0.043
			395	0.08	1.8	0.56	11.2	0.15	27.8	0.29	0.042
			1311[c]	0.02	1.7	0.59	11.4	0.13	28.3	0.28	0.045
			209[d]		1.7	0.66	14.0	0.30	28.3	0.04	0.026
			328[d]		1.7	0.65	12.6	0.29	26.8	0.06	0.026
EC DNA-9AA	50	1.2	209[c]	0.12	1.6	0.64	13.3	0.17	27.4	0.19	0.028
			417	0.06	1.7	0.63	12.9	0.17	27.6	0.20	0.028
ML DNA-9AA	72	1.1	400[e]	0.07							<0.002
10Me-9AA					16.2	1.00					0.926
CP DNA-10Me-9AA	30	1.6	200	0.10	2.2	0.33	10.8	0.25	26.3	0.43	0.090
			400	0.05	2.2	0.34	11.8	0.22	26.9	0.44	0.093
CT DNA-10Me-9AA	42	1.2	200	0.13	1.6	0.54	11.1	0.17	26.3	0.29	0.027
			400	0.06	1.7	0.54	12.3	0.15	26.4	0.31	0.029

[a] The solvent was 5 mM phosphate buffer (pH 6.9) at 25 °C, and the dye concentration was 10–13 μM. The decay was observed at 455 nm; the results obtained here are not dependent on the emission wavelength. χ^2 values ranged from 1.1 to 1.9. τ is given in nanoseconds, and the amplitudes (α's) are normalized to unity. [b] The percentage of free dye is equal to $100/[k_{app}(n_{app}/r - 1)]$, where r is the number of moles of dye bound per DNA phosphate group. [c] Kubota et al. (1979a). [d] Denatured DNA. [e] The fluorescence intensity was too weak to observe decay curves.

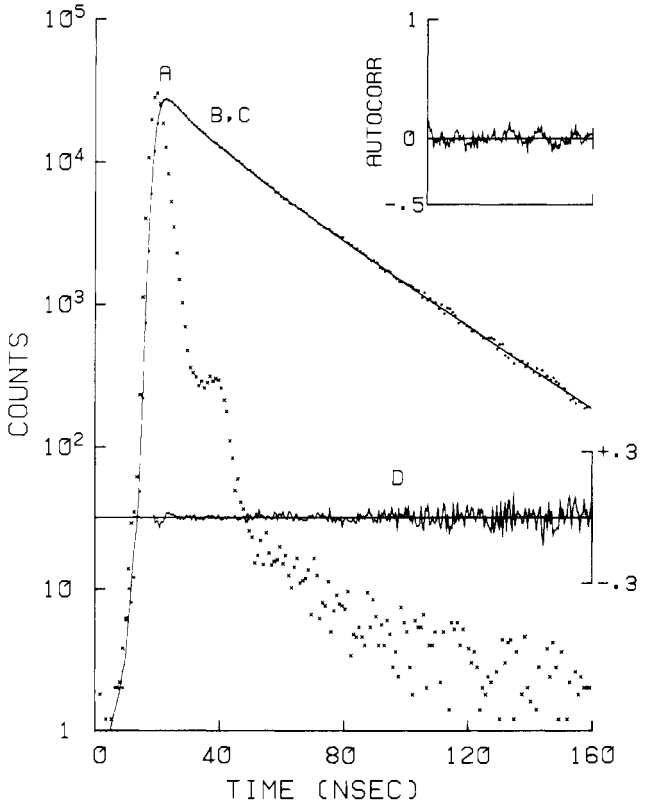

FIGURE 5: Three-component analysis of the fluorescence decay of the CP DNA–9AA complex. Conditions are as described for Figure 4. The computed decay curve is based on the following parameters: τ_1 = 2.2 ns, τ_2 = 12.2 ns, τ_3 = 29.2 ns, α_1 = 0.130, α_2 = 0.070, α_3 = 0.123, and χ^2 = 1.82. The amplitudes normalized to unity are α_1 = 0.40, α_2 = 0.22, and α_3 = 0.38.

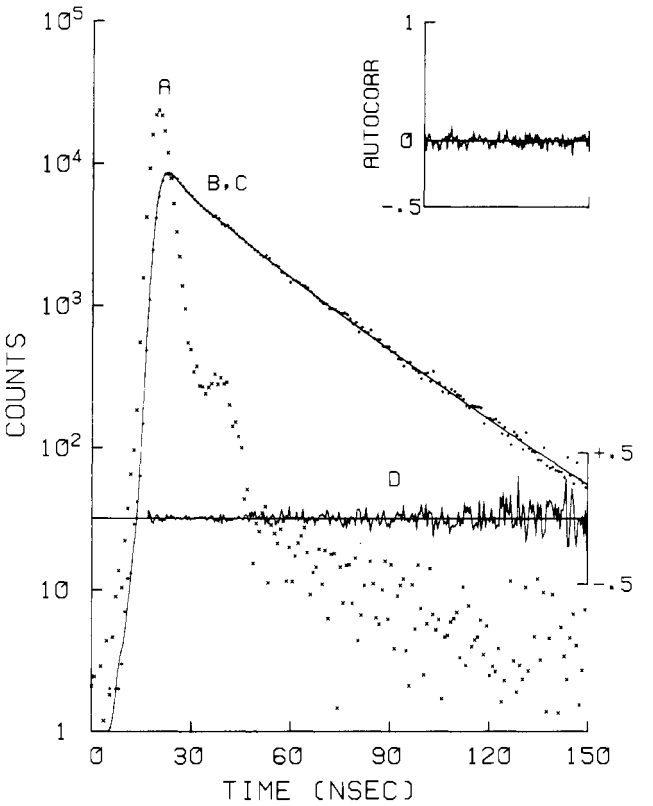

FIGURE 6: Three-component analysis of the fluorescence decay of the CT DNA–10Me-9AA complex (P/D = 400) in 5 mM phosphate buffer (pH 6.9) at 25 °C. The concentration of 10Me-9AA was 12 μM, and the decay was observed at 455 nm. Legends to each curve are as described for Figure 4. The computed decay curve is based on the following parameters: τ_1 = 1.7 ns, τ_2 = 12.3 ns, τ_3 = 26.4 ns, α_1 = 0.077, α_2 = 0.022, α_3 = 0.044, and χ^2 = 1.32. The amplitudes normalized to unity are α_1 = 0.54, α_2 = 0.15, and α_3 = 0.31.

ponential decay law, while Figure 5 indicates the best fit for a three-exponential decay law. The fit for the two-exponential components is seen to be poor, whereas that for the three-exponential components is excellent. Figure 6 also indicates that the decay kinetics of 10Me-9AA upon binding to DNA

obeys a three-exponential decay law. Typical sets of the decay parameters obtained for the DNA–dye complexes at high P/D values are summarized in Table I. In all cases, the χ^2 values, the weighed residuals, and the autocorrelation function of the residuals indicated that the data cannot be explained in terms of a two-exponential decay law but can be explained in terms of a three-exponential decay law. However, it should be emphasized that other more complex decay laws are not precluded because it is hard to analyze decay data in which two lifetimes are very close or one of amplitudes is very small (Isenberg, 1973; Gafni et al., 1975).

The accuracy expected from the analysis of decay data depends on the degree of correlation between the decay parameters (Isenberg, 1973; Gafni et al., 1975). In order to evaluate the accuracy, the following computation test was performed. A decay curve was synthesized by using the parameters shown in Table I and the other results presented in this paper, convolving with the apparatus response function $g(t)$ and adding photon counting noises. The synthetic decay curves were then analyzed by the method of nonlinear least squares. The original decay parameters were recovered within ±3% standard deviation. Accordingly, the origin of any uncertainty in the results presented here must be attributed to systematic errors in the instrument or impurities in the samples and not to errors introduced by the analysis method.

Very recently Duportail et al. (1977) reported that fluorescence decays of the DNA–9AA complexes obey a two-exponential decay law. The discrepancy between their results and ours may be ascribed to the following two points. The first is that no care was taken to eliminate anisotropic contributions to the observed decay in their studies. The second, more important point is that their fluorescence spectrum of the bound 9AA is different from ours. There is a peak around 420 nm in their spectrum [see Figure 7 in Duportail et al. (1977)]. In addition, their spectrum at 65 °C was distinct from ours which was very similar to spectra at 25 °C shown in Figure 2. Evidently the peak around 420 nm cannot be expected from the mirror-symmetry relation between the absorption and fluorescence bands (Figures 1 and 2). Therefore, the peak around 420 nm and the spectrum at 65 °C reported by Duportail et al. (1977) seems to arise from some impurity.

In order to elucidate the decay kinetics of the DNA–dye complexes and thus the nature of the emitting sites, the following studies have been undertaken.

Fluorescence Lifetimes and Quantum Yields of 9AA and 10Me-9AA upon Binding to Poly[d(A-T)] and Poly(dG)·Poly(dC). We first reexamined the fluorescence properties of the dye bound to poly[d(A-T)] and poly(dG)·poly(dC) which contain only one type of binding site (Kubota & Fujisaki, 1977). The fluorescence lifetimes and quantum yields are summarized in Table II. At P/D > 50 where conditions of complete binding are reached, the fluorescence decays of the poly[d(A-T)]–dye complexes follow a single-exponential decay law, and the lifetime and the quantum yield remain almost constant. It should be noted that the lifetime is very close to the component τ_3 shown in Table I.

On the other hand, the quantum yield for the poly(dG)·poly(dC)–9AA system decreases with increasing P/D until it attains zero at high P/D values (P/D > 100). The lifetime obtained at P/D = 21 is almost the same as that of the free 9AA. In view of the fact that fluorescence and fluorescence-excitation spectra of the poly(dG)·poly(dC)–9AA system are identical with the corresponding spectra of the free 9AA (Kubota & Fujisaki, 1977), it is concluded that the fluorescence in this case arises from the unbound 9AA. The quantum yield of 10Me-9AA bound to poly(dG)·poly(dC) is also zero (Table II). The results confirm that GC base pairs are responsible for the quenching sites of the dye (Kubota & Fujisaki, 1977; Kubota et al., 1978).

Table II: Fluorescence Lifetimes and Quantum Yields for 9AA and 10Me-9AA Bound to Poly[d(A-T)] and Poly(dG)·Poly(dC)[a]

system	$k_{app} \times 10^{-6}$ (M^{-1})	P/D	τ (ns)	ϕ
poly[d(A-T)]–9AA	1.3	136	31.3	0.73
		75	31.2	0.71
		50	30.9	0.70
poly(dG)·poly(dC)–9AA	0.9	130		≃0
		102[b]		<0.003
		51[b,c]		0.009
		21[c]	15.3	0.04
poly[d(A-T)]–10Me-9AA	1.4	141	29.5	0.63
		90	29.4	0.64
poly(dG)·poly(dC)–10Me-9AA	1.0	130		≃0

[a] The solvent was 5 mM phosphate buffer (pH 6.9) at 25 °C, and the dye concentration was 10–11 μM. The decay was observed at 455 nm. χ^2 values ranged from 1.3 to 1.8. [b] The fluorescence intensity was too weak to observe decay curves. [c] The contributions of free dye at P/D = 51 and P/D = 21 were estimated to be 0.9 and 2.6%, respectively; those for the other systems were below 0.5%.

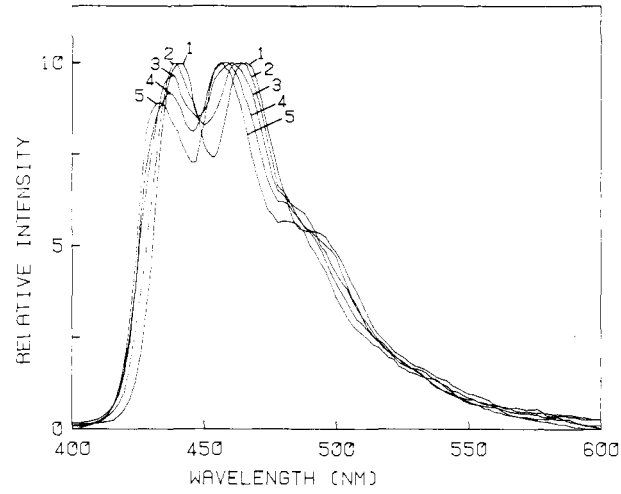

FIGURE 7: Fluorescence quantum spectra of the CT DNA–9AA complex (P/D = 220) as a function of ionic strength (I) at 25 °C: (1) $I \leq 0.02$; (2) $I = 0.05$; (3) $I = 0.1$; (4) $I = 0.2$; (5) $I = 0.4$. The concentration of 9AA was 11 μM, and the excitation wavelength was 390 nm. The desired ionic strength was achieved by using unbuffered NaCl solutions (0.001–0.4 M).

Effect of P/D and Ionic Strength on Fluorescence Decays. As can be seen in Table I, the values of τ_2 are close to the lifetime of the free dye (15.8 ns for 9AA and 16.2 ns for 10Me-9AA), and unbound dye, though very small in its amounts, is still present in the solutions of complexes. Since the quantum yield of the DNA–dye complex is considerably small as compared with that of the free dye (Table I), the question arises whether or not the unbound dye makes some contributions to the component τ_2 even at high P/D values. To answer the problem, we investigated fluorescence decay curves by first changing ionic strength (I = 0.001–0.4) at a high P/D value and by then changing P/D (P/D = 25–400) at an ionic strength of 0.01 (5 mM phosphate buffer).

Figure 7 shows the fluorescence spectra of the CT DNA–9AA complex (P/D = 220) obtained under various ionic strengths. Spectra are unchanged below I = 0.02. As ionic

Table III: Fluorescence Decay Parameters and Quantum Yields for CT DNA–9AA Complexes (P/D = 220) as a Function of Ionic Strength[a]

ionic strength	τ_1	α_1	τ_2	α_2	τ_3	α_3	φ
0.001	1.8	0.57	11.5	0.15	27.9	0.28	0.046
0.005	1.8	0.57	12.7	0.14	28.3	0.29	0.043
0.01	1.7	0.57	12.8	0.15	28.2	0.28	0.043
0.02	1.7	0.56	12.4	0.17	27.8	0.27	0.044
0.05	1.6	0.54	13.4	0.23	28.2	0.25	0.050
0.10	1.6	0.40	13.9	0.39	27.6	0.21	0.068
0.20	1.5	0.40	13.8	0.40	26.2	0.18	0.095

[a] The concentration of 9AA was 11 μM, and the decay was observed at 455 nm. The desired ionic strength was achieved by using unbuffered NaCl solutions (0.001–0.2 M). χ^2 values ranged from 1.1 to 1.8. τ is given in nanoseconds, and the amplitudes (α's) are normalized to unity.

strength is raised, fluorescence bands are progressively shifted toward shorter wavelengths, reflecting the increased contributions of the unbound 9AA. Nevertheless, in all cases, the best fit between the observed and calculated decay curves was obtained by three-component analysis (Table III). Theoretical and simulation considerations (Isenberg, 1973; Gafni et al., 1975) showed that it is difficult to analyze decay data in which two lifetimes are very close. Thus, the above result presumably is due to the closeness between the τ_2 value ($\tau_2 \simeq 12$ ns) and the lifetime of the free 9AA (15.8 ns). The τ_2 value obtained by three-component analysis increases with increasing ionic strength, corresponding to a continuous increase in the concentration of unbound dye. In conformity with changes in fluorescence spectra, the proportion of the α's is almost unchanged below $I = 0.02$ but further increase of ionic strength leads to the increase of the α_2 value (Table III).

Under conditions of P/D > 50 and ionic strength of 0.01 where not more than 0.6% of unbound dye is shown to be present, there was no significant effect of unbound dye on the absorption and fluorescence spectra. In this connection, we observe that the decay parameters obtained by three-component analysis are almost unchanged above P/D = 50 for each DNA (Table I). The increase of the α_2 value was observed at P/D < 50; this may be due to some contributions of unbound dye.

In view of these findings, it seems reasonable to conclude that under conditions of high P/D values (P/D > 100) and low ionic strength ($I < 0.02$), the effect of unbound dye is negligibly small and thus bound dye rather than unbound dye is responsible for the component τ_2.

Effect of DNA Denaturation on Fluorescence Decays. To study the effect of the conformational changes of DNA on the decay kinetics, we examined fluorescence decay curves of the heat-denatured DNA–9AA complexes. Fluorescence spectra measurements revealed that the concentration of unbound dye is not negligible even at high P/D values. However, three-component analysis of the decay data yielded the best result because of the reason mentioned above. Typical results obtained with denatured CT DNA are summarized in Table I. Compared with the results of native DNA (Table I), the component τ_3 dramatically decreases, while the component τ_1 still predominates; the increase of the α_2 values is ascribed to the contribution of unbound dye.

Nanosecond Time-Resolved Fluorescence Spectra. Finally, nanosecond time-resolved fluorescence spectra were measured in order to study any time-dependent interactions between the dye and its environment at the binding sites. It was found that the spectra exhibited no time dependence and were almost identical with the steady-state fluorescence spectra. In agreement with this finding, there were no significant changes in the decay parameters when the emission wavelength varied between 430 and 510 nm.

Discussion

It is found in the present study that the fluorescence decays of 9AA and 10Me-9AA upon binding to poly[d(A-T)] follow a single-exponential decay law but that those of the dye upon binding to DNA are complex. Our present criteria (χ^2, the weighed residuals, and the autocorrelation function of the residuals) show that the fluorescence decay curves of the DNA–dye complexes can be well resolved into three-exponential components corresponding to the short (τ_1), medium (τ_2), and long (τ_3) lifetimes. As is the case with any kinetic experiment, this does not rule out other decay laws which might also be found to agree with the data.

Since the absorption spectrum of bound dye overlaps its fluorescence spectrum (Figures 1 and 2), energy transfer between bound dye molecules might be possible as an explanation for the deviation of decay curves from single exponentiality (Kubota & Steiner, 1977a). On the basis of the Förster critical transfer distance (22 Å for 9AA and 24 Å for 10Me-9AA) (Förster, 1959), however, this appears unlikely at high P/D values. Actually, we observe that the fluorescence polarization (p) has a marked insensitivity to P/D (p = 0.22–0.24 for the DNA–9AA complexes at P/D > 50) and in addition, decay curves are also insensitive to P/D at high P/D values.

Nanosecond depolarization studies of the DNA–dye complexes showed that the change in the orientation of the intercalated dye is expected during the lifetime of the excited singlet state of the dye (Wahl et al., 1970; Kubota & Steiner, 1977b). However, the fact that nanosecond time-resolved fluorescence spectra of the dye bound to DNA are independent of time indicates that the structure of the DNA–dye complex is not substantially altered during the lifetime of the dye.

It can be seen in Table I that each fluorescence lifetime obtained by the three-component analysis is almost independent of the GC content of DNA, while the proportion of the amplitudes (α's) is dependent on it. It therefore seems reasonable to conclude that the fluorescence decay behavior of the DNA–dye complex is a result of the heterogeneity of the emitting sites. The association constants of the DNA–9AA and DNA–10Me-9AA complexes show no significant dependence on the GC content (Table I). Similar results have been obtained for the DNA–PF and DNA–acriflavin complexes (Ellerton & Isenberg, 1969; Chan & Van Winkle, 1969; Chan & McCarter, 1970). This suggests that most strong binding sites may have almost equal binding affinity for 9AA and 10Me-9AA as well as PF and acriflavin. It therefore seems likely that preferential binding to particular sites does not occur and the dye is randomly distributed among the available binding sites.

We first calculate the fraction of the emitting sites on the basis of fluorescence decay parameters and quantum yields given in Table I. If N is the total number of molecules which absorb light and N_i is the number of excited molecules with a lifetime τ_i, radiative lifetime τ_i^0, and quantum yield ϕ_i, the quantum yield of the system ϕ is given by eq 3 using the

$$\phi = \sum_{i=1}^{n}(N_i\phi_i)/N = \sum_{i=1}^{n}(N_i\tau_i/\tau_i^0)/N \qquad (3)$$

relation $\phi_i = \tau_i/\tau_i^0$. If the decay of the fluorescence intensity is represented by a sum of exponential functions like eq 2, the quantum yield of the ith component, ϕ_i, defined as the number

Table IV: Fraction of Emitting Sites[a]

DNA	GC (%)	dye	f	$f_{AT}{}^2$	$f_{AT}{}^3$	$f_{AT}{}^4$
CP DNA	30	9AA	0.31	0.490	0.343	0.240
		10Me-9AA	0.23			
T2 DNA	34	9AA	0.26	0.436	0.287	0.201
CT DNA	42	9AA	0.15	0.336	0.195	0.113
		10Me-9AA	0.10			
EC DNA	50	9AA	0.11	0.250	0.125	0.063

[a] The definitions of f, $f_{AT}{}^2$, $f_{AT}{}^3$, and $f_{AT}{}^4$ are described in the text.

of light quanta emitted by this component divided by N_i, is given by (Grinvald & Steinberg, 1974)

$$\phi_i = \int_0^\infty [\alpha_i \exp(-t/\tau_i)]\, dt/N_i = \alpha_i\tau_i/N_i \qquad (4)$$

Hence

$$N_i = \alpha_i\tau_i/\phi_i = \alpha_i\tau_i^0 \qquad (5)$$

The quantity $\sum_{i=1}^n N_i/N$ means the fraction of molecules occupying sites from which fluorescence may occur. We call this the fraction of the emitting sites and define it by f. Thus, we obtain

$$f = \frac{\sum_{i=1}^n N_i}{N} = \frac{\phi\sum_{i=1}^n N_i}{\sum_{i=1}^n (N_i\tau_i/\tau_i^0)} = \frac{\phi\sum_{i=1}^n (\alpha_i\tau_i^0)}{\sum_{i=1}^n (\alpha_i\tau_i)} \qquad (6)$$

The shapes or the maxima of the absorption and fluorescence spectra of the bound dye and the molar extinction coefficient of the bound dye show little dependence on the GC content of DNA. This suggests that the radiative lifetime of the bound dye is constant under a variety of circumstances, that is, irrespective of the nature of the binding sites. Actually we obtained the constant values 35.0 ± 1.0 and 37.0 ± 1.0 ns for the DNA–9AA and DNA–10Me-9AA complexes, respectively, according to the theory of Strickler & Berg (1962). If we call this constant τ^0 and normalize the original amplitude α_i in such a way that $\sum_{i=1}^n \alpha_i = 1$, we obtain

$$f = \frac{\phi\tau^0\sum_{i=1}^n \alpha_i}{\sum_{i=1}^n (\alpha_i\tau_i)} = \frac{\phi\tau^0}{\sum_{i=1}^n (\alpha_i\tau_i)} \qquad (7)$$

Table IV lists the values of f calculated by using eq 7. To avoid the error that might be introduced by the presence of unbound dye though very small in its amounts, we used the data obtained at sufficiently high P/D values (P/D > 200) in calculations of f. The results in Table IV indicate clearly that the value of f increases with decreasing GC content of DNA, providing additional evidence that AT and GC base pairs, respectively, play a role in the emitting and quenching sites. If we compare the value of f with the fractions of AT-AT ($f_{AT}{}^2$), AT-AT-AT ($f_{AT}{}^3$), and AT-AT-AT-AT ($f_{AT}{}^4$) sequences in DNA which were calculated by assuming that base pairs are located at random, it can be seen that f is not proportional to $f_{AT}{}^2$ but is roughly proportional to $f_{AT}{}^3$ for 9AA and $f_{AT}{}^4$ for 10Me-9AA (Table IV). This implies that AT-rich regions of DNA might be required for the emitting sites; this is in qualitative agreement with the previous finding (Kubota et al., 1978).

Next we discuss the nature of the emitting sites. Assuming that the radiative lifetime of the bound dye is constant and using the relation $\phi_i = \tau_i/\tau^0$, the ϕ_i values can be calculated. In view of the results shown in Table I and the ϕ_i values calculated, we can state that the emitting sites are composed of at least three classes having different quantum yields: for 9AA, (I) $\tau_1 = 2.0 \pm 0.3$ ns, $\phi_1 = 0.06 \pm 0.01$, (II) $\tau_2 = 12.3 \pm 0.7$ ns, $\phi_2 = 0.35 \pm 0.02$, and (III) $\tau_3 = 28.3 \pm 0.5$ ns, $\phi_3 = 0.81 \pm 0.02$, and for 10Me-9AA, (I) $\tau_1 = 1.9 \pm 0.3$ ns, $\phi_1 = 0.05 \pm 0.01$, (II) $\tau_2 = 11.5 \pm 0.6$ ns, $\phi_2 = 0.31 \pm 0.02$, and (III) $\tau_3 = 26.5 \pm 0.2$ ns, $\phi_3 = 0.72 \pm 0.01$.

The values of ϕ_3 and τ_3 are almost the same as the quantum yield and the lifetime of the poly[d(A-T)]–dye complex (Table II). Furthermore, there is a continuous increase of the α_3 value with decreasing GC content and its striking decrease in the case of denatured DNA which contains a small amount of nativelike parts (Table I). Therefore, it may be concluded that the class III is ascribed to the dye bound to AT-rich regions such as AT-AT–dye–AT-AT. As regards denatured DNA; our interpretation is based on the limited amounts of AT-rich regions, compared with those of native DNA.

In addition to the fully intercalated complex proposed by Lerman (1961, 1963), another type of complex is expected to occur. Dyes such as PF have been shown by the temperature-jump method to bind to DNA in two kinetically distinguishable stages (Li & Crothers, 1969; Ramstein & Leng, 1975). The resultant complex in the first stage corresponds to an external form of the complex in which the dye only partly overlaps the DNA base rings. This partly intercalated complex mainly occurs in the GC-rich regions of native DNA or in the single-strand denatured DNA as a precursor of the fully intercalated complex in the final stage (Ramstein & Leng, 1975). The possibility of partial intercalation has recently been demonstrated by X-ray crystallographic and proton magnetic resonance studies of complex formation between 9AA and dinucleotides or oligonucleotides (Sakore et al., 1977; Reuben et al., 1978).

Taking into account the fact that the components τ_1 and τ_2 are not observed for the poly[d(A-T)]–dye complex, GC pairs may play an important role in the classes I and II. If we do not distinguish AT pairs from TA pairs and GC pairs from CG pairs, there are three types of sites in DNA: AT-AT, AT-GC, and GC-GC sites. In view of the zero quantum yield obtained with poly(dG)·poly(dC) (Table II), the fluorescence of the dye bound to GC-GC sites may be totally quenched. It is also expected that the greater contact between the dye and guanine residues causes the more remarkable quenching of fluorescence. Therefore, the following explanation may be proposed for interpretation of our results. This would assume that the class I or II corresponds to different conformational states of the dye bound to AT-GC sites, fully intercalated or partly intercalated dye, and the class III corresponds to the dye intercalated in AT-AT sites. However, our results are not consistent with this interpretation, which predicts much larger values for ϕ and f since there exist a number of available AT-GC and AT-AT sites.

It has recently been found that GMP also quenches the fluorescence of 9AA and 10Me-9AA (Kubota, 1977; Kubota & Motoda, 1979) as well as PF (Badea & Georghiou, 1976). The encounter distance, R_0, between GMP and the dye is estimated to be ~8 Å (Badea & Georghiou, 1976; Y. Kubota and Y. Motoda, unpublished results) like other quenching systems (Mataga & Kubota, 1970); here, R_0 is the distance that the quenching process occurs with probability of 1. Furthermore, the quantum yields of the GMP–9AA and GMP–10Me-9AA complexes are found to be zero (Kubota & Motoda, 1979). If judged by this strong quenching ability of guanine residues or GC base pairs, we may expect that the

full intercalation in AT-GC sites leads to the total quenching of fluorescence and that the fluorescence of the partly intercalated dye in AT-GC sites or in AT-AT sites adjacent to GC pairs is appreciably quenched. In fact, the nearly zero quantum yield obtained with ML DNA (GC, 72%) is in accord with this prediction (Table I).

We propose here another explanation which would assume that the decay behavior of the DNA–dye complex has its origin in different binding sites, depending on the distance between the bound dye and the GC pair. In view of the facts that α_1 increases with increasing GC content and α_1 predominates in the case of denatured DNA (Table I) and due to the lowest quantum yield, the class I may be attributed to the partly intercalated dye in AT-GC sites. It can be seen that α_1 is rather high for T2 DNA, compared with its GC content (Table I). This may be due to glucosylation of T2 DNA which is known to increase the fraction of the external binding (Li & Crothers, 1969). From the earlier argument (see Results), the class II seems unlikely to result from the unbound dye although τ_2 is close to the lifetime of the free dye. The proportion of this site (α_2) is seen to be only slightly dependent on the base composition (Table I). In view of the fact that the fraction of GC-AT-AT sequences ($f_{GC}f_{AT}^2$) is insensitive to the GC content in its range of 30–50% ($f_{GC}f_{AT}^2$ = 0.125–0.148), we may attribute the class II to the partly intercalated dye in AT-AT sites adjacent to GC pairs. As mentioned above, the class III may be ascribed to the dye intercalated in AT-AT sites far from GC pairs. Perhaps the fully intercalated dye in AT-AT sites near GC pairs such as GC-AT-dye-AT might also contribute to the class III; in such a location, quenching interactions between the dye and guanine residues across one or more AT pairs seem unlikely. The relatively small values of f compared to the fraction of AT-GC sites (Table IV) imply that the proportion of the partly intercalated dye is considerably low; this is consistent with the finding that a small percentage of the total binding contributes to the external binding (Li & Crothers, 1969; Ramstein & Leng, 1975). At present, we have no direct experimental evidence to support either this interpretation or other mechanisms that might also be found to agree with our results. It is expected that further systematic studies using various acridine dyes will give a clue to the nature of the emitting sites.

The decay kinetics of the DNA–9AA and DNA–10Me-9AA complexes could be well described in terms of a three-exponential decay law, suggesting that there are at least three different emitting sites. It must be emphasized, however, that the actual decay law might be more complex since there would be many possibilities for the geometry of the bound dye and for the base sequences and also emphasized that the conclusion presented here is a possible inference.

Finally, it is interesting to compare the results of the mutagenic dye 9AA with those of the nonmutagenic dye 10Me-9AA. It can be seen in Tables I and IV that both results are very similar except that the f value, the quantum yield ϕ, and the component τ_3 for 10Me-9AA are somewhat smaller than those for 9AA. Possibly methylation of nitrogen in the acridine ring is responsible for these differences. Because of some steric hindrance of the methyl group against interactions between the dye and the DNA phosphate, we may expect that 10Me-9AA has a greater tendency to form the partly intercalated complex, compared with 9AA. Therefore, the possibility of radiationless transition by collisions with the surrounding solvent or quenching interactions with guanine residues would be expected to increase in the case of 10Me-9AA.

Schreiber & Daune (1974) found that the fluorescence of several acridine dyes having mutagenicity is quenched by GC pairs upon binding to DNA and attributed frame-shift mutations to the electronic modification of GC base pairs or guanine residues. In harmony with the results of the DNA–dye complexes obtained in the present study, however, we found that fluorescence quenching behavior of 10Me-9AA with purine mononucleotides is also very similar to that of 9AA (Kubota & Motoda, 1979). Our results imply that there might not be a direct relationship between the quenching behavior and the mutagenicity (Kubota et al., 1979b). It is expected that even a small change in the dye structure may cause a large change in the binding interaction of the dye with DNA (Peacocke, 1973). Perhaps the geometry of the intercalated dye may play a significant role in the biological activity of the dye.

Acknowledgments

We are indebted to Dr. Ludwig Brand for the method of decay analysis.

References

Albert, A., & Ritchie, B. (1943) *J. Chem. Soc.*, 458–462.
Badea, M. G., & Georghiou, S. (1976) *Photochem. Photobiol. 24*, 417–423.
Berlman, I. B. (1971) in *Handbook of Fluorescence Spectra of Aromatic Molecules*, 2nd ed., p 321, Academic Press, New York.
Bevington, P. R. (1969) in *Data Reduction and Error Analysis for the Physical Sciences*, pp 187–246, McGraw-Hill, New York.
Chan, L. M., & Van Winkle, Q. (1969) *J. Mol. Biol. 40*, 491–495.
Chan, L. M., & McCarter, J. H. (1970) *Biochim. Biophys. Acta 204*, 252–254.
Duportail, G., Mauss, Y., & Chambron, J. (1977) *Biopolymers 16*, 1397–1413.
Ellerton, N. F., & Isenberg, I. (1969) *Biopolymers 8*, 767–786.
Förster, Th. (1959) *Discuss. Faraday Soc. 27*, 7–17.
Gafni, A., Modlin, R. L., & Brand, L. (1975) *Biophys. J. 15*, 263–280.
Georghiou, S. (1977) *Photochem. Photobiol. 26*, 59–68.
Grinvald, A., & Steinberg, I. Z. (1974) *Anal. Biochem. 59*, 583–598.
Isenberg, I. (1973) *J. Chem. Phys. 59*, 5708–5713.
Kubota, Y. (1973) *Chem. Lett.*, 299–304.
Kubota, Y. (1977) *Chem. Lett.*, 311–316.
Kubota, Y., & Fujisaki, Y. (1977) *Bull. Chem. Soc. Jpn. 50*, 297–298.
Kubota, Y., & Steiner, R. F. (1977a) *Biophys. Chem. 6*, 279–289.
Kubota, Y., & Steiner, R. F. (1977b) *Bull. Chem. Soc. Jpn. 50*, 1502–1505.
Kubota, Y., & Motoda, Y. (1979) *Chem. Lett.*, 1375–1378.
Kubota, Y., Hirano, K., & Motoda, Y. (1978) *Chem. Lett.*, 123–126.
Kubota, Y., Motoda, Y., & Fujisaki, Y. (1979a) *Chem. Lett.*, 237–240.
Kubota, Y., Motoda, Y., Shigemune, Y., & Fujisaki, Y. (1979b) *Photochem. Photobiol. 29*, 1099–1107.
Lerman, L. S. (1961) *J. Mol. Biol. 3*, 18–30.
Lerman, L. S. (1963) *Proc. Natl. Acad. Sci. U.S.A. 49*, 94–102.
Lerman, L. S. (1964) *J. Cell. Comp. Physiol. 64 (Suppl. 1)*, 1–18.
Li, H. J., & Crothers, D. M. (1969) *J. Mol. Biol. 39*, 461–477.

Lochmann, E. R., & Micheler, A. (1973) in *Physico-Chemical Properties of Nucleic Acids* (Duchesne, J., Ed.) Vol. 1, pp 223–267, Academic Press, New York.
Mandell, J. D., & Hershey, A. D. (1960) *Anal. Biochem. 1*, 66–77.
Mataga, N., & Kubota, T. (1970) in *Molecular Interactions and Electronic Spectra*, pp 458–482, Marcel Dekker, New York.
Melhuish, W. H. (1961) *J. Phys. Chem. 65*, 229–235.
Orgel, A., & Brenner, S. (1961) *J. Mol. Biol. 3*, 762–768.
Pachman, U., & Rigler, R. (1972) *Exp. Cell Res. 72*, 602–608.
Peacocke, A. R. (1973) in *Heterocyclic Compounds: Acridines* (Acheson, R. M., Ed.) Vol. 9, pp 723–757, Interscience, New York.
Peacocke, A. R., & Skerrett, J. N. H. (1956) *Trans. Faraday Soc. 52*, 261–279.
Ramstein, J., & Leng, M. (1975) *Biophys. Chem. 3*, 234–240.
Reuben, J., Baker, B. M., & Kallenbach, N. R. (1978) *Biochemistry 17*, 2915–2919.
Sakore, T. D., Jain, S. C., Tsai, C. C., & Sobell, H. M. (1977) *Proc. Natl. Acad. Sci. U.S.A. 74*, 188–192.
Schreiber, J. P., & Daune, M. (1974) *J. Mol. Biol. 83*, 487–501.
Shinitzky, M. (1972) *J. Chem. Phys. 56*, 229–235.
Spencer, R. D., & Weber, G. (1970) *J. Chem. Phys. 52*, 1654–1663.
Strickler, S. J., & Berg, R. A. (1962) *J. Chem. Phys. 37*, 814–822.
Thomes, J. C., Weill, G., & Daune, M. (1969) *Biopolymers 8*, 647–659.
Tubbs, R. K., Ditmars, W. E., & Van Winkle, Q. (1964) *J. Mol. Biol. 9*, 545–557.
Wahl, Ph., Paoletti, J., & Le Pecq, J. B. (1970) *Proc. Natl. Acad. Sci. U.S.A. 65*, 417–421.
Wahl, Ph., Auchet, J. C., & Donzel, B. (1974) *Rev. Sci. Instrum. 45*, 28–32.
Weisblum, B., & de Haseth, P. L. (1972) *Proc. Natl. Acad. Sci. U.S.A. 69*, 629–632.

In Vivo Effects of Intercalating and Nonintercalating Drugs on the Tertiary Structure of Kinetoplast Deoxyribonucleic Acid†

Jean Bénard* and Guy F. Riou

ABSTRACT: The kinetoplast DNA (kDNA) of cultured *Trypanosoma cruzi* consists mostly in a large network of numerous minicircular molecules (~25 000), with a very low degree of superhelicity. When the intercalating drugs ethidium bromide and 9-hydroxyellipticine were added to the growth medium in concentrations producing trypanocidal effects, the superhelicity of the kDNA was significantly increased. In contrast, the nonintercalating drug berenil had no effect on the superhelicity of kDNA. In the kDNA extracted from trypanosomes resistant to ethidium bromide or 9-hydroxyellipticine, those drugs induce similar effects, although to a lesser extent than in the wild strain.

In unicellular flagellates of the order Kinetoplastida, a modified region of the mitochondrial apparatus, the kinetoplast, contains DNA (kDNA) at high concentration [see reviews by Simpson (1972) and Englund (1979)]. As shown by electron microscopy, the kDNA of *Trypanosoma cruzi* consists in a complex network of more than 25 000 covalently closed minicircles of 1.4 kilobase pairs and longer molecules in small proportion (Riou & Delain, 1969a). These molecules are apparently held together by topological interlocking. In other species of trypanosomes, the longer molecules have been identified as "maxicircles" and can be removed by some restriction endonucleases (Kleisen et al., 1976; Riou & Saucier, 1979).

A number of studies have established that the kDNA of trypanosomes may be considered as a target for DNA-binding drugs [for a review, see Steinert (1971)]. Ethidium bromide, a representative intercalating dye (Crawford & Waring, 1967; Le Pecq & Paoletti, 1967) has trypanocidal activity (Watkins & Woolfe, 1956). This drug binds to kDNA, inhibits its replication, and induces its progressive and complete loss (Riou 1968, 1970; Riou et al., 1980). The intercalating drug 9-hydroxyellipticine has high affinity for DNA (Festy et al., 1971; Le Pecq et al., 1974), decreases the rate of growth of trypanosomes (Bénard & Riou, 1976), and affects the in vitro kDNA transcription process (Bénard & Riou, 1977). Ethidium bromide and 9-hydroxyellipticine have no base composition specificity. Berenil, a nonintercalating drug which preferentially binds to AT-rich DNA (Festy et al., 1970a), inhibits kDNA replication and is also a trypanocidal drug (Brack et al., 1972; Newton, 1972).

Recently we have determined by sedimentation velocity–ethidium bromide titration (Wang, 1969) the degree of superhelicity of closed minicircles in the network of *T. cruzi*: the normal superhelix density of kDNA is very low and varies with the physiological state of the trypanosomes in different phases of growth (Bénard et al., 1979).

Direct measurements of the in vivo binding of intercalating drug to kDNA cannot be done because it is not possible to obtain intact kinetoplasts from *T. cruzi* and because the intercalation process is reversible. An approach consists in measuring the changes in conformation of the minicircles after treatment of the trypanosomes with drugs. Since intercalating drugs unwind the DNA helix (Wang, 1974) and assuming the presence of in vivo enzymatic nicking–closing activities, an increase in the number of superhelical turns per DNA minicircle would be an index of in vivo intercalation. This indirect procedure has been successfully used by Smith et al. (1971)

† From the Laboratoire de Pharmacologie Moléculaire, Institut Gustave Roussy, 94800 Villejuif, France. *Received February 28, 1980.*

0006-2960/80/0419-4197$01.00/0